V.M. Gun'ko

THEORETICAL ANALYSIS OF ADSORPTION OF VARIOUS COMPOUNDS ONTO HYDROPHILIC AND HYDROPHOBIC SILICAS COMPARED TO ACTIVATED CARBONS

Chuiko Institute of Surface Chemistry of National Academy of Sciences of Ukraine
17 General Naumov Str., Kyiv, 03164, Ukraine, E-mail: vlad_gunko@ukr.net

The aim of this study was to analyze various theoretical models (clusters, systems with periodic boundary conditions) and methods, which could be applied to investigate the adsorption phenomena and for better interpretation of the experimental data. The density functional theory (DFT) and semiempirical (PM7) methods were used to model the adsorption phenomena at a surface of fumed nanooxides, silica gels, activated carbons, etc. The main idea is that appropriate theoretical analysis allows a deeper insight into interfacial phenomena related to the structure & properties of the adsorption layers vs. the textural and other characteristics of adsorbents. Comparison of the theoretically calculated characteristics with experimental ones can allow more accurate interpretation of the effects observed in various experiments on the adsorption phenomena. It was established that polarization of nonpolar and polar molecules adsorbed onto a polar surface and charge (& proton) transfer play an important role, as well as confined space effects. It enhances the interaction energy of adsorbed molecules bound to a solid surface and affects the surface orientation of adsorbed molecules, as well the behavior of the adsorption layer vs. temperature, pressure or concentration, as well other conditions. Surface hydrophobization reduces the interaction energy for both polar and nonpolar adsorbates. Adsorbates clusterization reduces the average energy of interaction of the adsorption layer with a surface per a molecule. The charge transfer is observed for both polar and nonpolar molecules interacting with polar surface functionalities. The mostly strong interfacial effects changing the behavior of the adsorption layer are observed upon proton transfer to the adsorbed molecules or vice versa. Variation in orientation of adsorbed molecules results in overestimation of the specific surface area estimated using a fixed value of surface area occupied by a probe molecule (e.g. 0.162 nm^2 for N_2).

Keywords: quantum chemical methods, ab initio and DFT methods, semiempirical methods, silica models, activated carbon models, adsorption models

INTRODUCTION

Investigations of adsorption phenomena using various experimental methods typically give average and sometimes too general pictures with no some important and detailed information [1–13]. Additional information could be obtained using theoretical modelling of the adsorption phenomena using appropriate methods and models [13–18]. Accurate information could be obtained using *ab initio* (with Møller-Plesset theory corrections) and DFT with large basis sets and consideration of the effects of temperature (with various dynamic approaches), media (with solvation models), lateral interactions of adsorbates, sizes of solid particle models (cluster approach) or expanded cells (periodic boundary conditions), *etc*. However, the mostly accurate methods/models of the adsorption phenomena need great computational resources (e.g., supercomputers). Some restrictions in the latter lead to a problem

of a choice of appropriate models and methods/basis sets [13–18].

There are many factors affecting the adsorption and related phenomena: (i) morphology, structure, and texture of adsorbents; (ii) molecular structure and molecular weight of adsorbates; (iii) polarity of adsorbate molecules and adsorbent surface, charge and proton transfer, interaction energy, and changes in the Gibbs free energy upon adsorption; (iv) orientation of adsorbate molecules at a surface and lateral interactions; (v) confined space effects and changes in a molecule shape due to adsorption; (vi) temperature, pressure in a gas phase or concentration in a liquid phase, and time of adsorption; (vii) co-adsorption of various adsorbates, solvation-desolvation and competition effects; (viii) effects of equilibrium and non-equilibrium conditions; (ix) mechanical or other external actions on the systems, *etc*. [1–13]. These numerous factors can lead to

complicated interpretation of some experimental results, but theoretical investigations can help to get over the difficulty [13]. Therefore, the aim of this study was to analyze various theoretical models and methods to be applied on the adsorption phenomena.

MODELS AND QUANTUM CHEMICAL METHODS

In the models used, dozens of polar (H_2O, NH_3, CO_2) and nonpolar (C_6H_6, N_2, CH_4 or fragments of polydimethylsiloxane, PDMS, poly(vinyl alcohol), PVA, poly(ethylene glycol), PEG) molecules and some their mixtures were adsorbed onto hydrophilic silica (models with 22-44 tetrahedra in DFT and hundreds of tetrahedra in PM7) and hydrophobic silica clusters with attached dimethylsilyl or trimethylsilyl groups. Quantum chemical calculations were carried out using the DFT method with a hybrid functional ωB97X-D and the cc-pVDZ or aug-cc-pVTZ basis sets using the Gaussian 09 (D.01) [19] and GAMESS 18.R3 [20] program suits. The solvation effects were analyzed using the SMD method [21, 22]. The gauge-independent atomic orbital (GIAO) method [19] was used to calculate the NMR spectra of certain systems. Larger structures (up to 18000 atoms) were calculated using semiempirical PM7 method (MOPAC 2016) [23]. Visualization of the calculation results was carried out using several programs described in detail elsewhere [24–26].

RESULTS AND DISCUSSION

Silica samples could be represented by relatively large porous particles such as silica gels or nonporous nanoparticles (NPNP) such as fumed nanosilica (Fig. 1). These silicas can have similar values of the specific surface area (S_{BET}), but they are characterized by very different pore size distributions (PSD) (Fig. 1 *d*). The PSD of fumed silica is broad because it deals with the textural porosity caused by voids between NPNP in their aggregates and agglomerates of aggregates (ANPNP). The total pore volume (V_p) evaluated from the nitrogen adsorption is much lower than the empty volume ($V_{em} = 1/\rho_b - 1/\rho_0$, where ρ_b and ρ_0 are the bulk and true densities of samples) in the nanosilica powder, since V_{em} can reach 24.5 cm^3/g for A-300 at $\rho_b \approx 0.04$ g/cm^3, but the value of V_p is typically less than 1 cm^3/g [13, 27, 28]. This difference in the particulate

morphology and texture of silicas can result in certain differences in the behavior of adsorbates bound in pores of silica gel or voids between NPNP in nanosilica. Therefore, the used models of nanosilica particles (Fig. 2) and pores in silica gels (Fig. 3) reflect main textural features of these adsorbents.

Activated carbons (AC) as well silicas are most important adsorbents used in various industry, medical, and scientific applications [1–13]. AC and silicas are characterized by very different texture and surface nature. These differences should be reflected in the particulate models used (Figs. 2–4).

One of important factors on the analyses of the adsorption phenomena is that the results on, *e.g.*, the textural characterization depend on the characteristics not only of adsorbents but also adsorbates. For example, the PSD of a set of AC calculated using the nitrogen and benzene as probes differ (Fig. 5) because nitrogen and benzene molecules are of different sizes and nature. Thus, any adsorbate using as an adsorption probe can affect the adsorption results that lead to a certain ambiguity in the adsorbent characterization.

Nonpolar nitrogen molecules are polarized and weakly charged due to interactions with any adsorbent (Tables 1 and 2). However, the confined space effects are absent for silica NPNP (Fig. 2 *a*). Therefore, the calculated interaction energy is relatively small since it corresponds to the second peak of the adsorption energy distributions (AED) *f*(*E*) [13] upon interaction of molecules only with one surface (Figs. 6–8). The AED are characterized by several peaks (Figs. 6–8). The first peak at the *E* values close to the heat of vaporization of nitrogen molecules (5.56 kJ/mol) corresponds to the adsorbed molecules (AM), which do not sense the pore walls, *i.e.*, they adsorbed in broad pores far from the pore walls. The second *f*(*E*) peak corresponds to AM sensing only one pore wall in broad mesopores. In narrow pores, AM can weakly and strongly sense two walls that results in the third *f*(*E*) peak. In nanopores, AM strongly sense two walls that corresponds to the fourth *f*(*E*) peak (Figs. 6–8).

Besides the confined space effects in pores of different sizes and the effects caused by the surface structure and composition, there is an effect of orientation of adsorbed molecules. The latter depends not only on the nature of a solid

surface but also on lateral interactions (Fig. 9). Therefore, for silicas and AC, the surface area occupied by N$_2$ molecule $\sigma_{\text{eff}} = (0.85 \div 0.90) \times \sigma_0$,

thus, the value of S_{BET} estimated using $\sigma_0 = 0.162$ nm^2 is always overestimated.
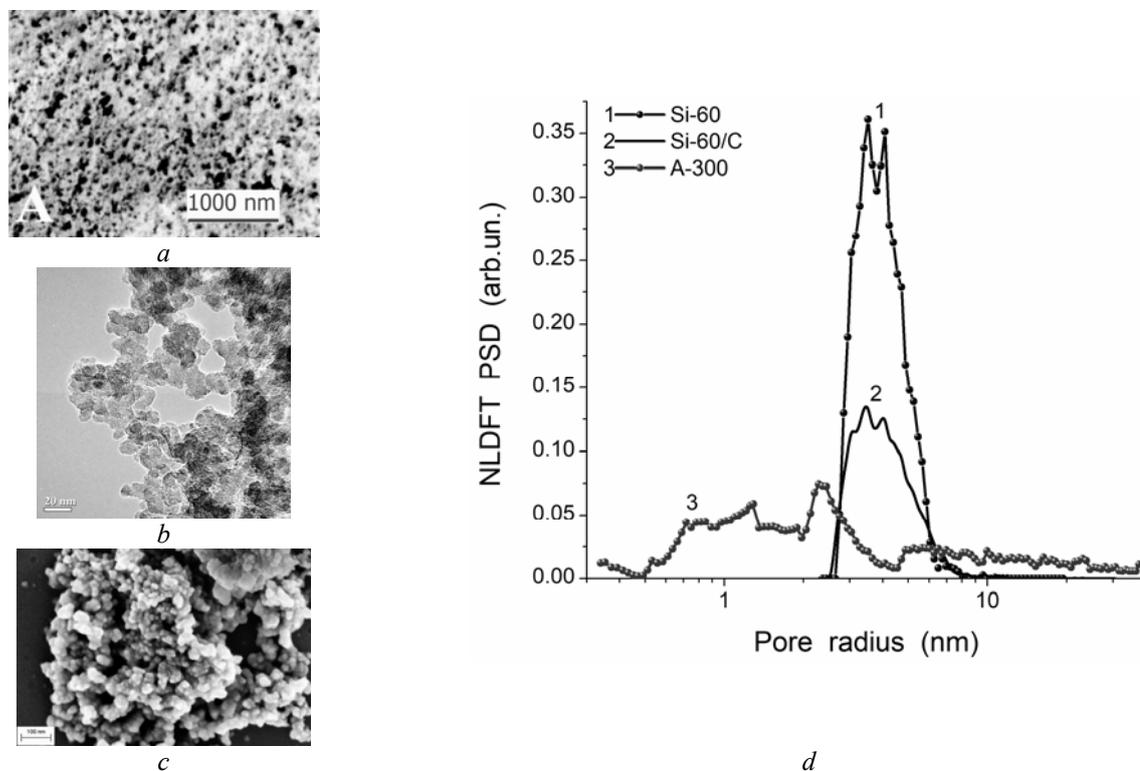
Fig. 1. TEM (*a, b*) and SEM (*c*) images of (*a*) silica gel Si-60 initial with porous particles of 0.2–0.5 mm in size at $S_{\text{BET}} = 357$ m^2/g; (*b, c*) fumed silica A-300 with nonporous nanoparticles of 9.3 nm in average diameter at $S_{\text{BET}} = 294$ m^2/g; (*d*) NLDFT pore size distributions of Si-60 initial (*1*) and covered by nonporous carbon particles of 0.1–2.0 μm in diameter (*2*), and fumed silica A-300 initial (*3*)
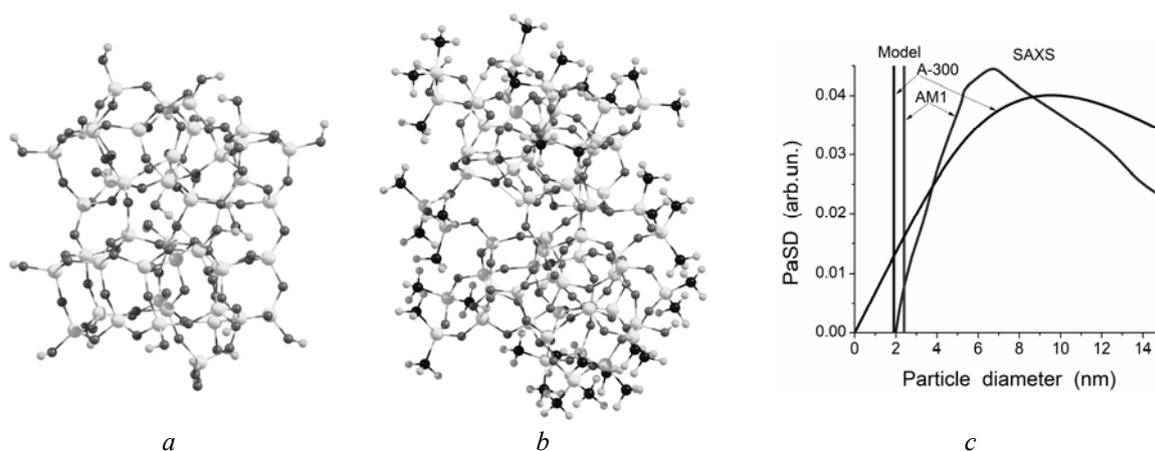

Fig. 2. Models of hydrophilic (*a*) and hydrophobic (*b*) silica nanoparticles: (*a*) 44 tetrahedrons (SiO$_{4/2}$) with 24OH groups, (*b*) 44 (SiO$_{4/2}$)+19(=Si(CH$_3$)$_2$)+5OH modelling A-300 hydrophobized by dimethyldichlorosilane, hydrolyzed and lateral-crosslinked (hydrophobic nanosilica AM1); geometry was optimized using DFT ωB97X-D/cc-pVDZ; (*c*) particle size distributions (PaSD) of A-300 and AM1 based on SAXS data
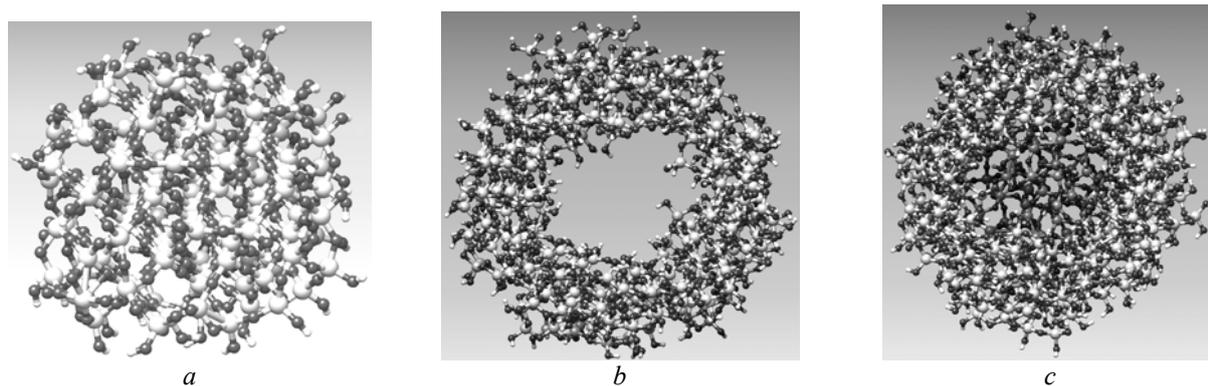
Fig. 3. Models of nonporous (*a*) and porous (*b, c*) particles of silica at (*a*) particle diameter *d* = 2.2 nm, (*b, c*) *d* = 3.6 nm, pore diameter = 1.2 nm, (*c*) one-side closed pore of 4 nm in depth
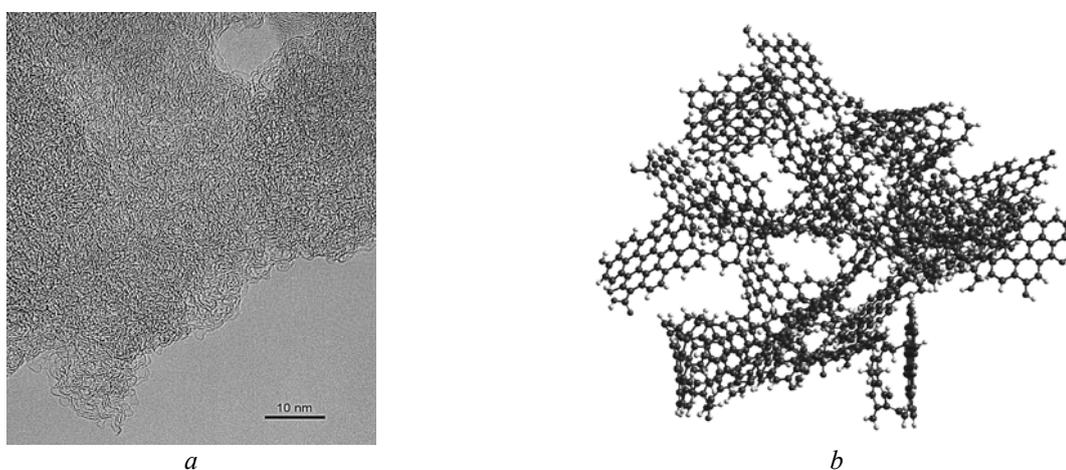

Fig. 4. (*a*) HRTEM image of AC with 50% burn-off, (*b*) AC model (~5 nm in size, 1589 atoms) used in adsorption studies (PM7 geometry)
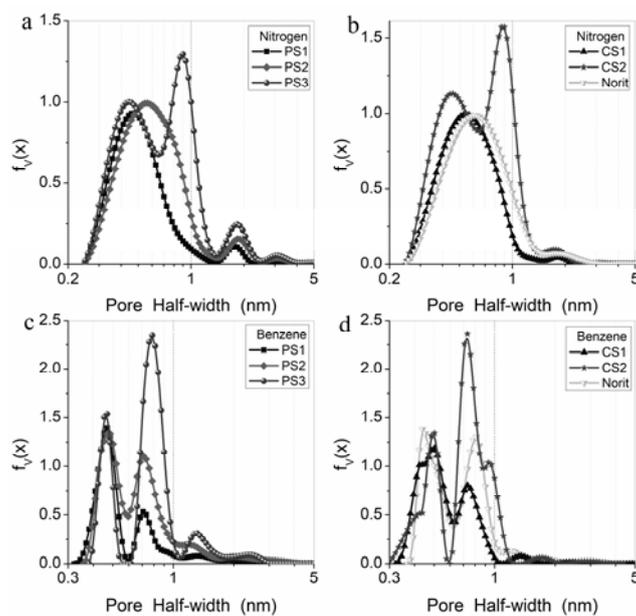

Fig. 5. Textural characteristics of various AC estimated from nitrogen (*a, b*) and benzene (*c, d*) adsorption (PSD are probe dependent) [13]
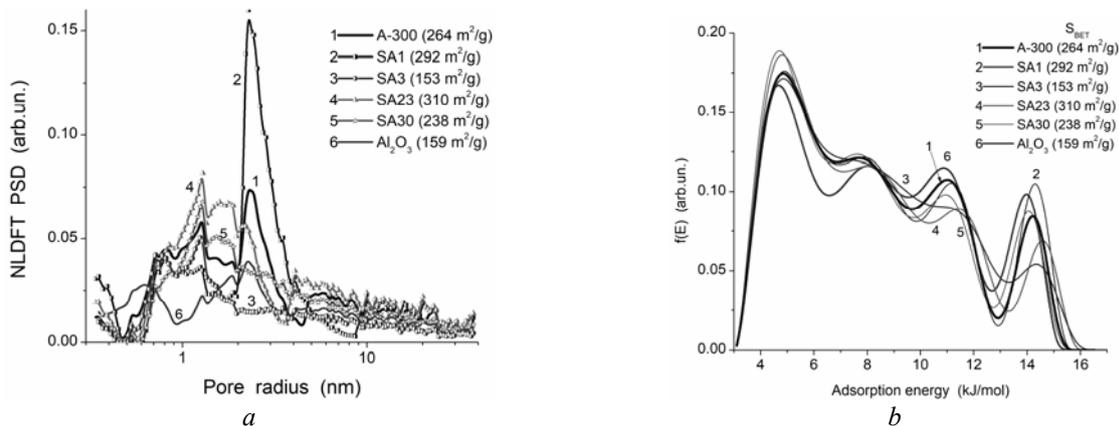
Fig. 6. PSD (*a*) of silica (*S*), alumina (*A*), and mixed SA oxides and nitrogen adsorption energy using Fowler-Guggenheim kernel of integral eq. (*b*)
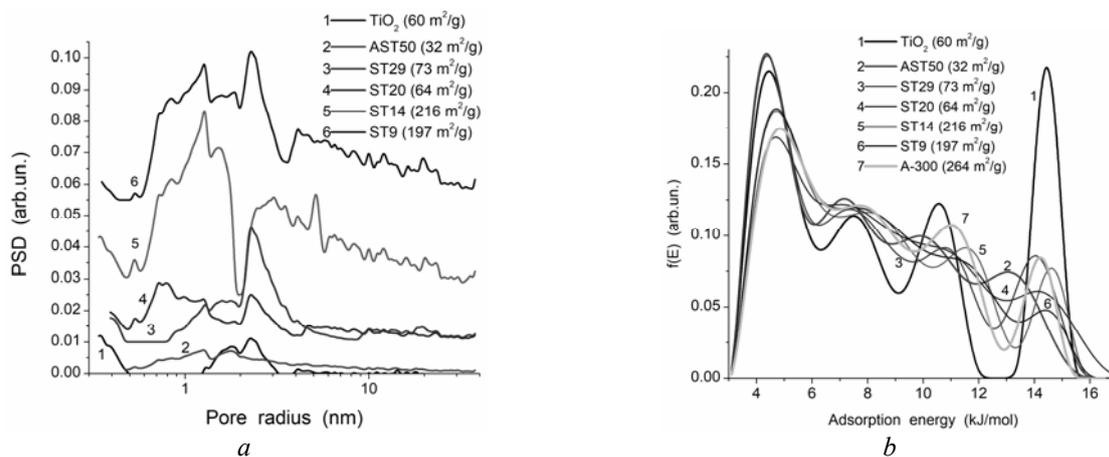
Fig. 7. NLDFT PSD (*a*) and nitrogen adsorption energy distributions (*b*) of titania and mixed silica/titania (ST)
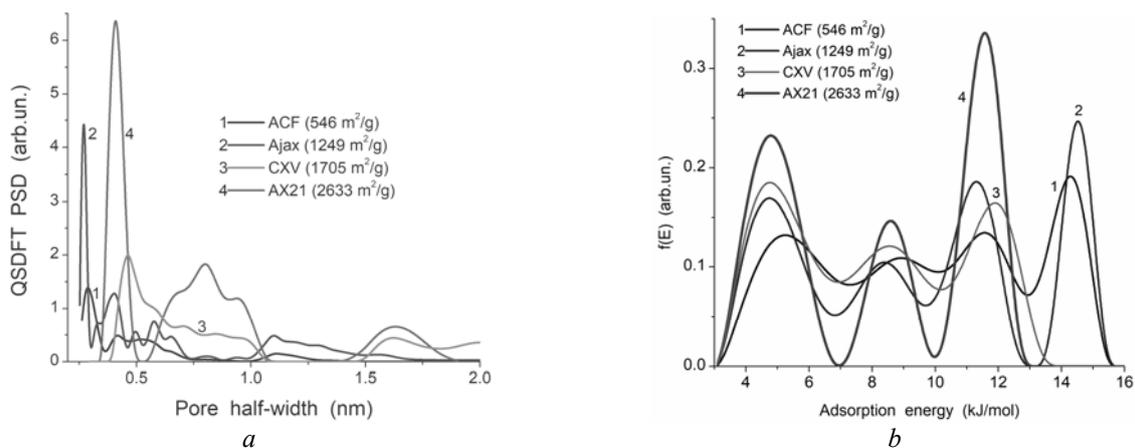
Fig. 8. QSDFT PSD (*a*) of carbons and nitrogen adsorption energy distributions (*b*)

Table 1. Adsorption energy ($\Delta E_{1,\mathrm{BSSE}}$) and charge transfer ($\Delta q_1$) per a molecule for various probes adsorbed onto silica (ωB97X-D/cc-pVDZ)
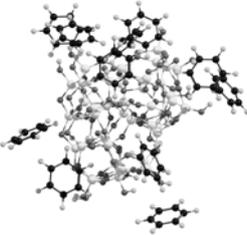
| Adsorbate	$-\Delta E_1$ (kJ/mol)	Δq_1 (a.u.)
$11C_6H_6$		
	32.8	-0.033
$40N_2$		
	6.9	0.019
$37CO_2$		
	14.5	0.013
$34NH_3\ NH_4^+$		
	62.8	0.068
$41H_2O\ H_3O^+$		
	74.5	0.067
$17H_2O\ 32NH_3\ 2NH_4^+$		
	63.0	0.068
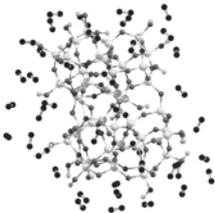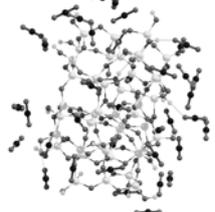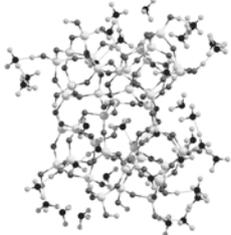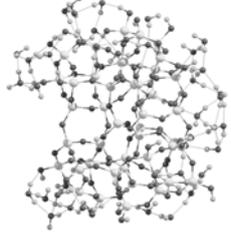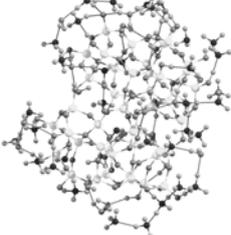
Table 2. Adsorption energy (ΔE_1) per a molecule of various probes adsorbed onto silica and AC (PM7)

Adsorbent	Adsorbate	$-\Delta E_1$ (kJ/mol)
Silica	$37CO_2$	13.5
Silica	$35NH_3$	27.3
AC	$227C_6H_6$	4.0
AC	$99N_2$	4.6
AC	$1397H_2O$	6.3
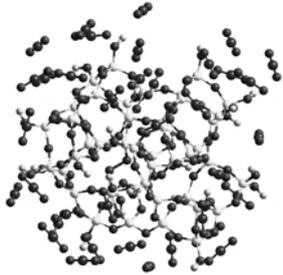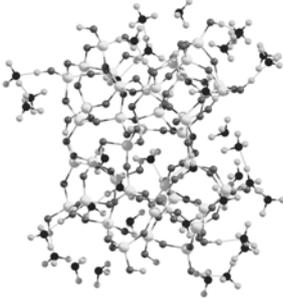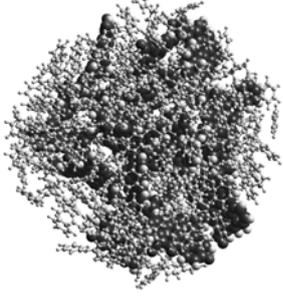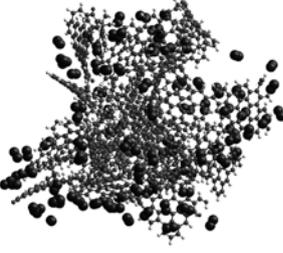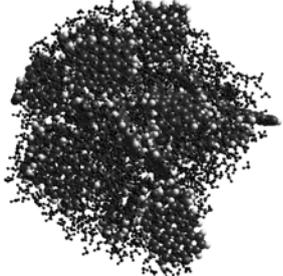
The effects of confined space, surface nature and specific area, as well the nature and structure of adsorbates (X) strongly affect the results of adsorption with respect to estimation of the specific surface area. The values of $S_{BET,X}$ could be overestimated (due to very strong interaction with active surface sites (strong Brønsted and Lewis acid surface sites in mixed fumed metal oxides, FMO) leading to conformational changes of adsorbed molecules) and underestimated (due to weak interaction of adsorbed molecules with weak surface sites, NPNP aggregation, which increases with decreasing size of FMO NPNP, reducing accessibility of the surface for larger molecules) (Fig. 9).

An increase in the number of adsorbed molecules of water (Fig. 10 *a*) or other molecules (Fig. 10 *b*) typically leads to reduction of the interaction energy and charge transfer per a molecule because only molecules from the first adsorption layer strongly sense the surface in contrast to distant molecules. For polar molecules interacting with hydroxylated surface, it is possible proton transfer, which strongly changes the characteristics of the adsorption layer. Note that for alumina/silica cluster (Si/Al = 38/6) with $40H_2O + 2H_3O^+$, $\Delta E_{1,w} = -77.3$ kJ/mol and $\Delta q_{1,w} = 0.086$ and these values are greater than that for similar pure silica cluster with bound water due to increased polarization effects.
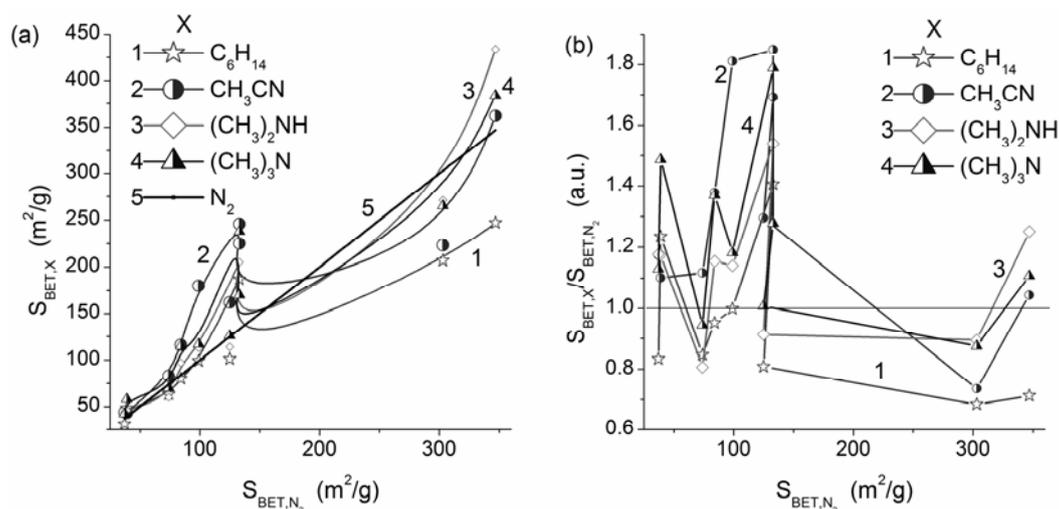
Fig. 9. Specific surface area (S_{BET}) *vs.* surface and adsorbed probe (X) structures: relationships between the $S_{BET,N2}$ and (*a*) $S_{BET,X}$ or (*b*) $S_{BET,X}/S_{BET,N2}$ values for silica, alumina, titania and mixed fumed oxides [29–31]
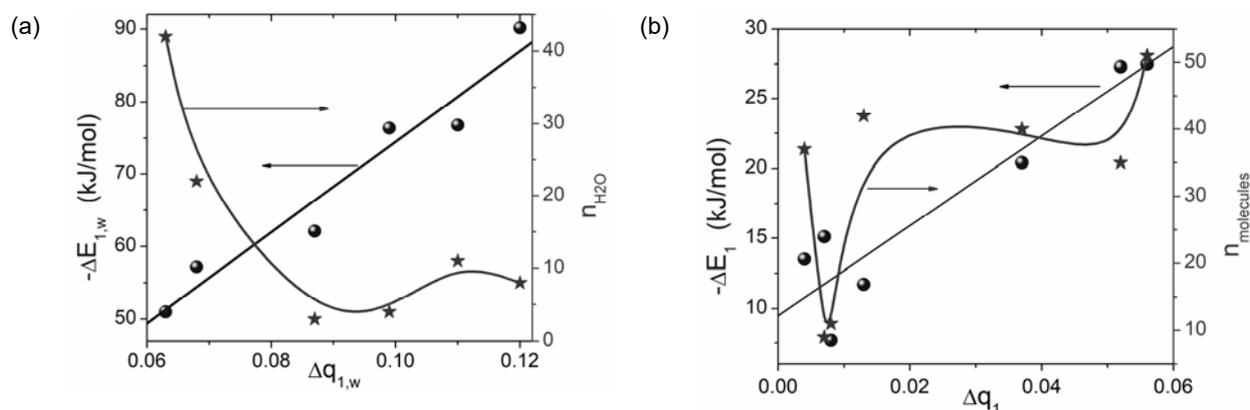

Fig. 10. (*a*) DFT (ωB97X-D/cc-pVDZ) results for bound water and (*b*) PM7 results for interaction energy *vs.* charge transfer upon adsorption of N_2, NH_3, CO_2, H_2O, $NH_3 + H_2O$, and C_6H_6 (various numbers of molecules) onto hydrophilic and hydrophobic silica nanoparticles (per a molecule)

These phenomena are well seen in the ^{1}H NMR spectra of bound adsorbates (Fig. 11) showing strong downfield shifts (peaks at 9–14 ppm) because of reducing proton shielding. This effect is observed in the NMR spectra of both liquid and solid acids [13]. The confined space effects appear in the ^{1}H NMR spectra of water bound in pores or onto NPNP (Fig. 12). The former leads to the downfield shift in comparison to the latter. However, surface modification, *e.g.* hydrophobization of a silica surface [32–36] or compaction of FMO [37], changes the confined space effects for both polar (Fig. 13) and nonpolar (Figs. 14 and 15) adsorbates. This is especially characteristic for water, which tends to form clusters at both polar or nonpolar surfaces. However, the hydrophobization strongly reduces the interaction energy even in nanopores (Fig. 15).


a   *b*
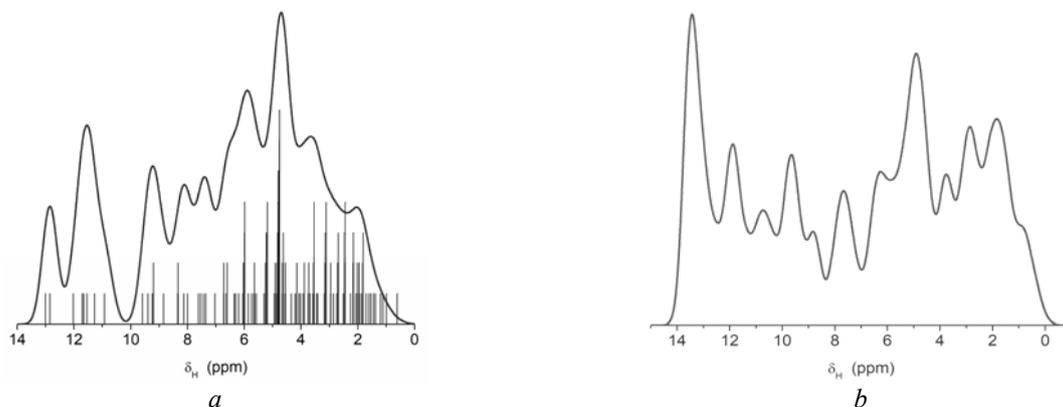
Fig. 11. ^{1}H NMR spectra of (*a*) a cluster with H$^+$ transfer 44(SiO$_{4/2}$) with 23(OH)(O$^-$) + 39H$_2$O+OH$_3^+$ $\Delta E_{BSSE,1}$ = -74.5 kJ/mol, Δq_t = 2.81, Δq_1 = 0.067. Structures around H$_3^+$O, strong H-bonds, H-bonds, weak H-bonds, and free OH; (*b*) effects of H$^+$ transfer: 44(SiO$_{4/2}$) with 22(OH)@2(O$^-$)+17H$_2$O+32NH$_3$ +2NH$_4^+$ $\Delta E_{BSSE,1}$ = -60 kJ/mol (both ads) and -67.8 kJ/mol (ads1+ads2), Δq_t = 3.46, Δq_1 = 0.068 (*b*). Structures around NH$_4^+$, strong H-bonds, H-bonds, weak H-bonds, and free OH (GIAO/ωB97X-D/cc-pVDZ)
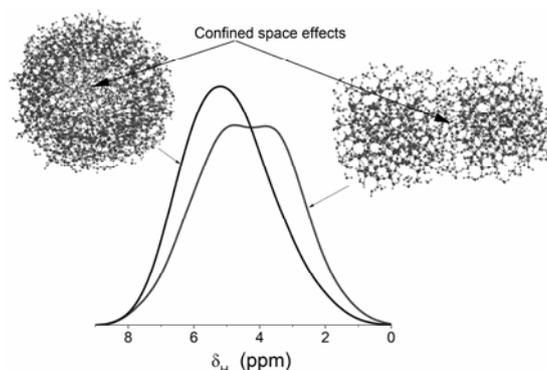

Fig. 12.   Theoretical ^{1}H NMR spectra of water bound to porous and nonporous nanoparticles (PM7)

The surface structure and texture (*i.e.* confined space effects), as well conditions (temperature, pressure, time of adsorption, co-adsorbates), strongly affect the dynamic behavior of adsorbates (Figs. 16–18). Clearly, physical (non-activated) adsorption decreases with increasing temperature (Fig. 16). However, an increase in pressure enhances the adsorption due to faster return of molecules from the gaseous phase into the adsorption layer. This effect is well seen on comparison of the dynamic behavior of water molecules bound to silica located in a periodic box (the molecules can return to the surface) and upon desorption in open space (with no return of the molecules to the surface) (Fig. 17 *a*). If the molecules adsorbed in pores that their evaporation is restricted (Fig. 17 *b*, *c*) especially in semi-closed pore (Fig. 17 *d*).

Fig. 13. Clustered water adsorption onto hydrophobic AM1, $\Delta E_{1,w}$ = -29.0 kJ/mol (with BSSE correction, ωB97X-D/cc-pVDZ), -15.1 kJ/mol (PM7), $\Delta q_{1,w}$= 0.033 (ωB97X-D/cc-pVDZ), 0.007 (PM7)
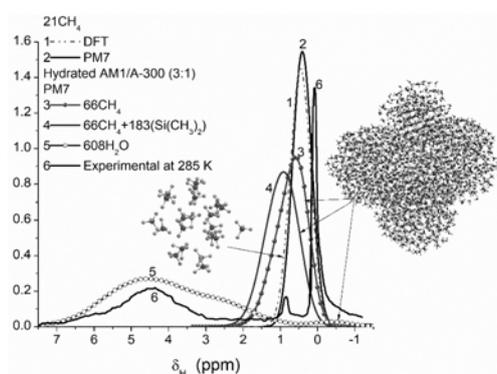
Fig. 14. Theoretical (21CH$_4$ - curves 1 (GIAO/ωB97X–D/cc–pVDZ) and 2 (PM7), a model AM1/A-300 (3:1, with 3 AM1 particles (each with 61 groups of Si(CH$_3$)$_2$ and 123 SiO$_{4/2}$ tetrahedra) and one silica particles (123 SiO$_{4/2}$ tetrahedra) and bound 608H$_2$O and 66CH$_4$) shown in insert was calculated using PM7 method – curves 3-5) and experimental (curve 6, AM1/A-300 (3:1) at *h* = 0.1 g/g and 285 K) ^{1}H NMR spectra
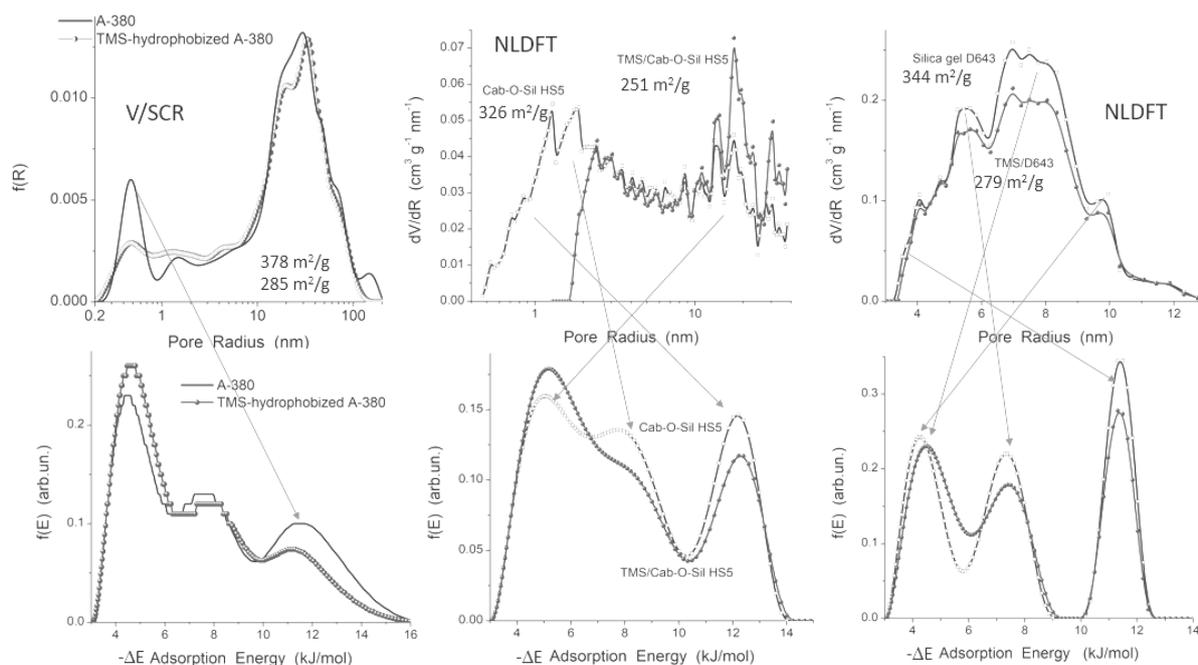
Fig. 15. Effects of silica hydrophobization on nitrogen adsorption energy distributions

T = 0K ⟶ 170 K, 11 ps ⟶ 250 K, 5 ps ⟶ 310 K, 5 ps
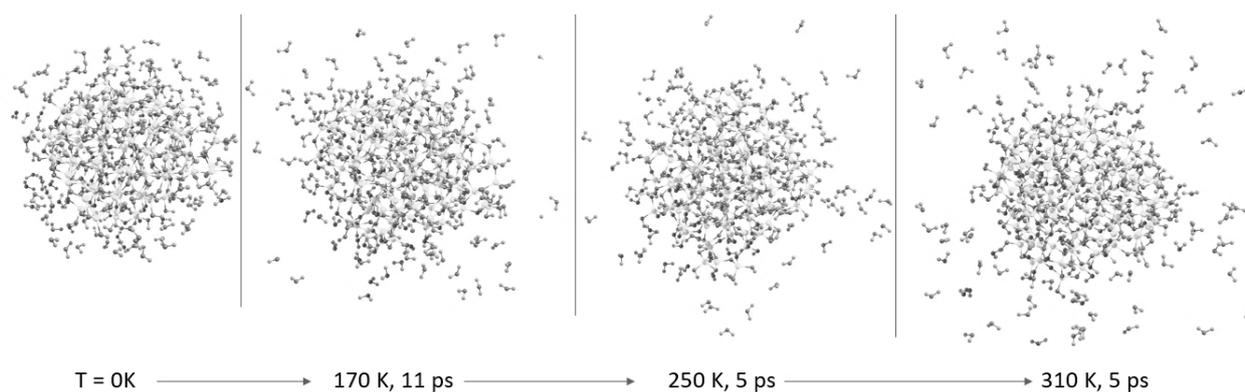
Fig. 16. MD model of water bound to silica *vs.* temperature: MM+ force field calculations with periodic boundary conditions, water shell with 107 H_2O around silica nanoparticles heated at various temperatures (with no confined space effects). This behavior of water molecules results in weak adsorption onto non-aggregated nonporous silica nanoparticles. Nanoparticles aggregation (*i.e.* appearance of the textural porosity) leads to a certain increase in the adsorption of water onto fumed silica, but it is much smaller than that adsorbed onto porous micro/macroparticles (*e.g.* silica gel)
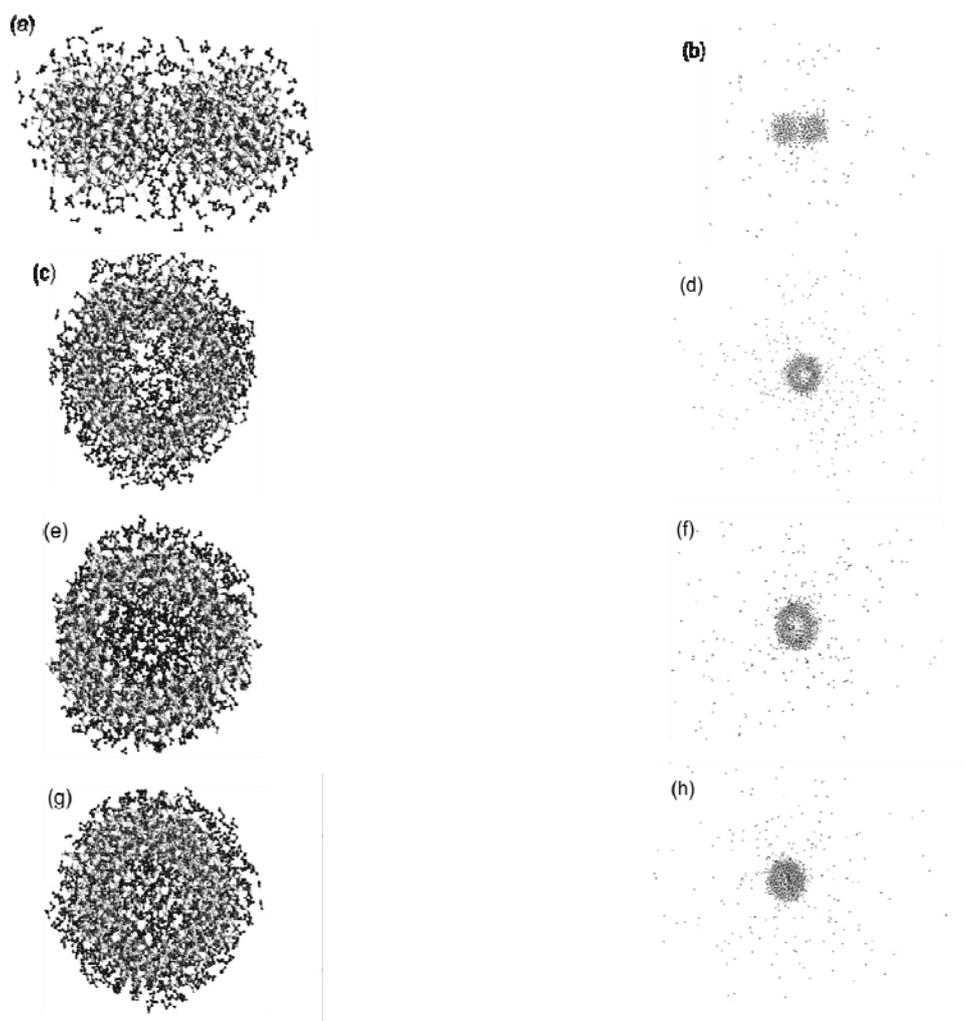
Fig. 17. MD/force field (MM+) calculations of dehydration of silicas at 293 K for 10 ps: (*a, b*) nanosilica, (*c, d*) hydration of outer and inner surface of silica gel with open pore; (*e, f*) more stronger hydration of pore of silica gel; and (*g, h*) silica gel with one-side-closed pore filled by adsorbed water
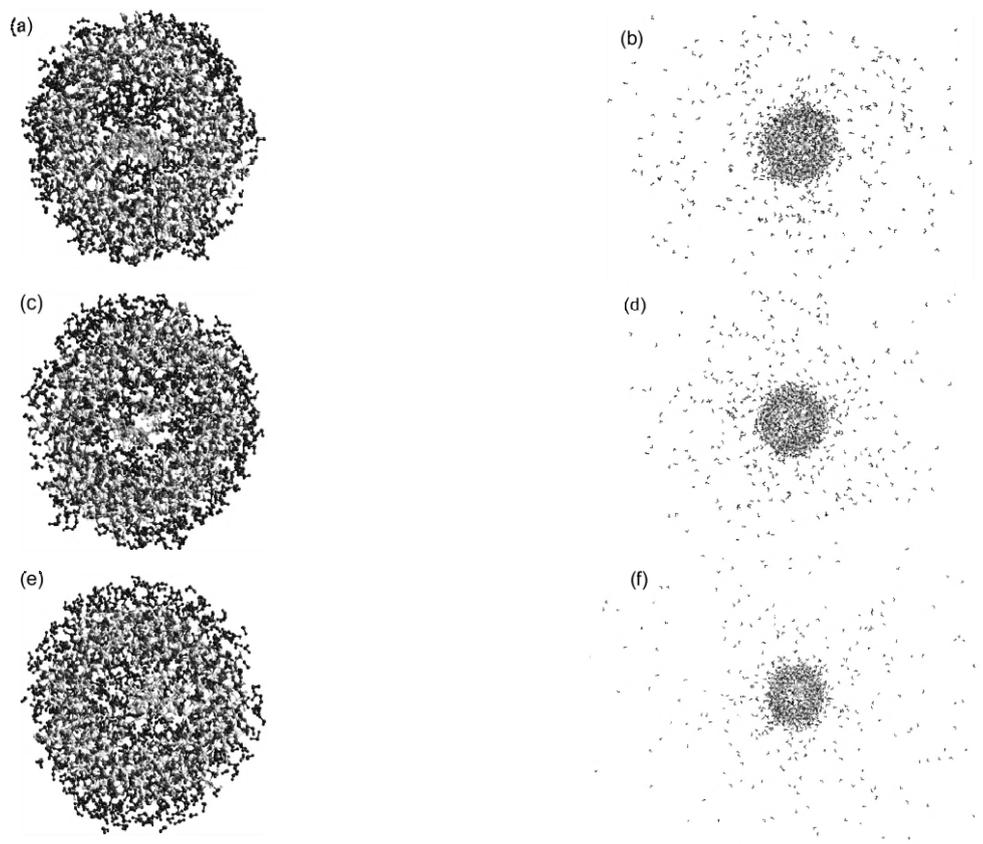
Fig. 18. Effects of co-adsorbates: MD/force field (MM+) calculations of dehydration of silica gel particle at 293 K for 10 ps with polymers located in pore: (*a*, *b*) PVA (two fragments), (*c*, *d*) PEG (two fragments); (*e*, *f*) PDMS (one fragment)

Desorption of water molecules decreases if they co-adsorbed with both polar or nonpolar polymers in pores (Fig. 18) due to enhanced confined space effects. Polar polymers enhance the adsorption energy that also reduced the evaporation of water molecules from pores.

CONCLUSION

Theoretical analysis allows a deeper insight into interfacial phenomena related to the structure & properties of the adsorption layers *vs.* the textural and other characteristics of adsorbents. Comparison of the theoretically calculated characteristics with experimental ones can allow more accurate interpretation of the effects observed in various experiments on the adsorption phenomena. Polarization of nonpolar and polar molecules adsorbed onto a polar surface and charge (& proton) transfer play an important role, as well confined space effects. It increases the interaction energy of adsorbed

molecules bound to a solid surface and affects the surface orientation of adsorbed molecules, as well the behavior of the adsorption layer *vs.* temperature, pressure or concentration, as well as other conditions. Surface hydrophobization reduces the interaction energy for both polar and nonpolar adsorbates. Clusterization of adsorbates reduces the average energy of interaction of the adsorption layer with a surface per a molecule. The charge transfer is observed for polar and nonpolar molecules interacting with polar surface functionalities. The strong effects change the behavior of the adsorption layer are observed upon proton transfer to the adsorbed molecules or *vice versa*. Variation in orientation of adsorbed molecules results in overestimation of the specific surface area estimated using a fixed value of surface area occupied by a probe molecule (*e.g.* 0.162 nm^2 for N$_2$).

Теоретичний аналіз адсорбції різних сполук на гідрофільних та гідрофобних кремнеземах у порівнянні з активованим вугіллям

В.М. Гунько

Інститут хімії поверхні ім. О.О. Чуйка Національної академії наук України
вул. Генерала Наумова, 17, Київ, 03164, Україна, vlad_gunko@ukr.net

Мета роботи полягала у аналізі теоретичних моделей (кластерів, періодичних граничних умов) та методів, які можуть бути використані для вивчення явищ адсорбції та для кращої інтерпретації експериментальних даних. Теорія функціоналу густини (DFT, ωB97X-D) та напівемпіричні (PM7) методи використали для моделювання адсорбційних явищ на поверхні пірогенних нанооксидів, силікагелю, активованого вугілля тощо. Головна ідея полягала в тому, що теоретичний аналіз дозволяє більш глибоко розуміти міжфазні явища, що пов'язані зі структурою та властивостями адсорбційних шарів в залежності від структурних та інших особливостей адсорбентів. Порівняння теоретично розрахованих особливостей з експериментальними може дозволити більш точну інтерпретацію ефектів, які спостерігають в різних експериментах по адсорбційним явищам. Було визначено, що поляризація неполярних та полярних молекул, адсорбованих на полярній поверхні, та перенесення заряду (протонів) відіграє важливу роль, як і ефекти обмеженого простору. Це збільшує енергію взаємодії адсорбованих молекул, зв'язаних з твердою поверхнею, і визначає поверхневу орієнтацію адсорбованих молекул, а також поведінку адсорбційного шару при змінах температури, туску чи концентрації, а також інших умов. Гідрофобізація поверхні зменшує енергію взаємодії і для полярних, і для неполярних адсорбатів. Кластеризація сорбатів зменшує середню енергію взаємодії адсорбційного шару з поверхнею у перерахунку на одну молекулу. Перенесення заряду спостерігається для полярних і неполярних молекул, які взаємодіють з полярними поверхневими функціональними групами. Ці сильні ефекти змінюють поведінку адсорбційного шару особливо при перенесенні протонів на адсорбовані молекули чи навпаки. Зміни в орієнтації адсорбованих молекул призводить до переоцінки посадочного майданчика, яку займає молекула, і використання постійного значення цієї величини (наприклад, $0.162\,нм^2$ для N_2) призводить до переоцінювання питомої поверхні адсорбента.

Ключові слова: квантовохімічні методи, неемпіричні та ТФГ методи, напівемпіричні методи, моделі кремнеземів, моделі активованого вугілля, моделі адсорбції

Теоретический анализ адсорбции разных соединений на гидрофильных и гидрофобных кремнеземах в сравнении с активированным углем

В.М. Гунько

Институт химии поверхности им. А.А. Чуйко Национальной академии наук Украины
ул. Генерала Наумова, 17, Киев, 03164, Украина, vlad_gunko@ukr.net

Цель роботы состояла в анализе теоретических моделей (кластеров, периодических граничных условий) и методов, которые могут быть применимы для изучения явлений адсорбции и для лучшей интерпретации экспериментальных данных. Теорию функционала плотности (DFT, ωB97X-D) и полуэмпирические (PM7) методы использовали, чтобы смоделировать адсорбционные явления на поверхности пирогенных нанооксидов, силикагелей, активированного угля и т.д. Главная идея состоит в том, что теоретический анализ позволяет более глубоко понимать межфазные явления, связанные со структурой и свойствами адсорбционных слоев в зависимости от структурных и других особенностей адсорбентов. Сравнение теоретически рассчитанных особенностей с экспериментальными может позволить более точную интерпретацию эффектов, наблюдаемых в различных экспериментах по адсорбционным явлениям. Было установлено, что поляризация неполярных и полярных молекул, адсорбированных на полярной поверхности, и перенос заряда (протонов) играет важную роль, также, как и эффекты ограниченного пространства. Это увеличивает энергию взаимодействия адсорбированных молекул, связанных с твердой поверхностью, и определяет поверхностную ориентацию адсорбированных молекул, а также поведение адсорбционного слоя при изменениях температуры, давления или концентрации, а также других условий. Гидрофобизация

поверхность уменьшает энергию взаимодействия и для полярных, и для неполярных адсорбатов. Кластеризация адсорбатов уменьшает среднюю энергию взаимодействия адсорбционного слоя с поверхностью в пересчете на одну молекулу. Перенос заряда наблюдается для полярных и неполярных молекул, взаимодействующих с полярными поверхностными функциональными группами. Эти сильные эффекты изменяют поведение адсорбционного слоя особенно при переносе протонов на адсорбированные молекулы или наоборот. Изменение в ориентации адсорбированных молекул приводит к переоценке посадочной площадки, занятой молекулой, и использование постоянного значения этой величины (например, 0.162 нм^2 для N_2) приводит к переоценке удельной поверхности адсорбента.

Ключевые слова: квантовохимические методы, неэмпирические и ТФП методы, полуэмпирические методы, модели кремнеземов, модели активированного угля, модели адсорбции

REFERENCES

1. Gregg S.J., Sing K.S.W. *Adsorption, Surface Area and Porosity*. 2nd ed. (London: Academic Press, 1982).
2. Adamson A.W., Gast A.P. *Physical Chemistry of Surface*. 6th ed. (New York: Wiley, 1997).
3. Iler R.K. *The Chemistry of Silica*. (Chichester: Wiley, 1979).
4. Legrand A.P. *The Surface Properties of Silicas*. (New York: Wiley, 1998).
5. Bergna H.E., Roberts W.O. *Colloidal Silica: Fundamentals and Applications*. (Boca Raton: CRC Press, 2006).
6. Ghosh S.K. *Functional Coatings*. (Weinheim: Wiley-VCH Verlag GmbH, 2006).
7. Tapia O., Bertrán J. *Solvent Effects and Chemical Reactivity*. (New York: Kluwer Academic Publishers, 2000).
8. Somasundaran P. *Encyclopedia of Surface and Colloid Science*. Third Edition. (Boca Raton: CRC Press, 2015).
9. Henderson M.A. The interaction of water with solid surfaces: fundamental aspects revisited. *Surf. Sci. Rep.* 2002. **46**(1–8): 1.
10. Birdi K.S. *Handbook of Surface and Colloid Chemistry*. Third edition. (Boca Raton: CRC Press, 2009).
11. Al-Abadleh H.A., Grassian V.H. Oxide surfaces as environmental interfaces. *Surf. Sci. Rep.* 2003. **52**(3–4): 63.
12. Chandler D. Interfaces and the driving force of hydrophobic assembly. *Nature*. 2005. **437**: 640.
13. Gun'ko V.M., Turov V.V. *Nuclear Magnetic Resonance Studies of Interfacial Phenomena*. (Boca Raton: CRC Press, 2013).
14. Dykstra C.E., Frenking G., Kim K.S., Scuseria G.E. *Theory and Applications of Computational Chemistry, the First Forty Years*. (Amsterdam: Elsevier, 2005).
15. Canuto S. *Solvation Effects on Molecules and Biomolecules. Computational Methods and Applications*. (Dordrecht: Springer, 2008).
16. Schleyer P.v.R. *Encyclopedia of Computational Chemistry*. (New York: John Wiley & Sons, 1998).
17. Cramer C.J. *Essentials of computational chemistry: theories and models*. Second ed. (Chichester, UK: John Wiley & Sons, Ltd, 2008).
18. Yang K., Zheng J., Zhao Y., Truhlar D.G. Tests of the RPBE, revPBE, τ-HCTHhyb, ωB97X-D, and MOHLYP density functional approximations and 29 others against representative databases for diverse bond energies and barrier heights in catalysis. *J. Chem. Phys.* 2010. **132**(16): 164117.
19. Frisch M.J., Trucks G.W., Cheeseman J.R., Scalmani G., Caricato M., Hratchian H.P., Li X., Barone V., Bloino J., Zheng G. Gaussian 09, Version D.01. Gaussian Inc. Wallingford CT 2013.
20. Schmidt M.W., Baldridge K.K., Boatz J.A., Elbert S.T., Gordon M.S., Jensen J.H., Koseki S., Matsunaga N., Nguyen K.A., Su S., Windus T.L., Dupuis M., Montgomery J.A. Jr. General atomic and molecular electronic structure system. *J. Comput. Chem*. 1993. **14**(11): 1347.
21. Marenich A.V., Cramer C.J., Truhlar D.G. Universal solvation model based on solute electron density and on a continuum model of the solvent defined by the bulk dielectric constant and atomic surface tensions. *J. Phys. Chem. B*. 2009. **113**(18): 6378.
22. Marenich A.V., Cramer C.J., Truhlar D.G. Performance of SM6, SM8, and SMD on the SAMPL1 test set for the prediction of small-molecule solvation free energies. *J. Phys. Chem. B*. 2009. **113**(14): 4538.
23. Stewart J.J.P. MOPAC2016. Stewart Computational Chemistry. 2019. http://openmopac.net
24. Dennington R., Keith T., Millam J. GaussView, Version 5.09. Semichem Inc., Shawnee Mission KS, 2013.
25. Zhurko G.A., Zhurko D.A. Chemcraft (version 1.8). 2019. http://www.chemcraftprog.com
26. Hanwell M.D., Curtis D.E., Lonie D.C., Vandermeersch T., Zurek E., Hutchison G.R. Avogadro: an advanced semantic chemical editor, visualization, and analysis platform. *J. Chem. Inf.* 2012. **4**(17): 1.
27. Gun'ko V.M. Composite materials: textural characteristics. *Appl. Surf. Sci.* 2014. **307**: 444.

28. Gun'ko V.M., Turov V.V., Gorbyk P.P. *Water at the Interfaces*. (Kyiv: Naukova Dumka, 2009). [in Russian].
29. Gun'ko V.M., Turov V.V., Zarko V.I., Goncharuk O.V., Pahklov E.M., Skubiszewska-Zięba J., Blitz J.P. Interfacial phenomena at a surface of individual and complex fumed nanooxides. *Adv. Colloid Interface Sci.* 2016. **235**: 108.
30. Gun'ko V.M. Interfacial phenomena: effects of confined space and structure of adsorbents on the behavior of polar and nonpolar adsorbates at low temperatures. *Current Physical Chemistry.* 2015. **5**(2): 137.
31. Gun'ko V.M. Modeling of interfacial behavior of water and organics. *J. Theor. Comput. Chem.* 2013. **12**(07): 1350059.
32. Gun'ko V.M., Pakhlov E.M., Goncharuk O.V., Andriyko L.S., Nychiporuk Yu.M., Balakin D.Yu., Sternik D., Derylo-Marczewska A. Nanosilica modified by polydimethylsiloxane depolymerized and chemically bound to nanoparticles or physically bound to unmodified or modified surfaces: Structure and interfacial phenomena. *J. Colloid Interface Sci.* 2018. **529**: 273.
33. Gun'ko V.M., Turov V.V., Pakhlov E.M., Krupska T.V., Borysenko M.V., Kartel M.T., Charmas B. Water interactions with hydrophobic versus hydrophilic nanosilica. *Langmuir.* 2018. **34**(40): 12145.
34. Gun'ko V.M., Turov V.V., Krupska T.V., Pakhlov E.M. Behavior of water and methane bound to hydrophilic and hydrophobic nanosilicas and their mixture. *Chem. Phys. Lett.* 2017. **690**: 25.
35. Turov V.V., Gun'ko V.M., Pakhlov E.M., Krupska T.V., Tsapko M.D., Charmas B., Kartel M.T. Influence of hydrophobic nanosilica and hydrophobic medium on water bound in hydrophilic components of complex systems. *Colloids Surf. A.* 2018. **552**: 39.
36. Gun'ko V.M., Pakhlov E.M., Goncharuk O.V., Andriyko L.S., Marynin A.I., Ukrainets A.I., Charmas B., Skubiszewska-Zięba J., Blitz J.P. Influence of hydrophobization of fumed oxides on interactions with polar and nonpolar adsorbates. *Appl. Surf. Sci.* 2017. **423**: 855.
37. Gun'ko V.M., Turov V.V., Pakhlov E.M., Krupska T.V., Charmas B. Effect of water content on the characteristics of hydro-compacted nanosilica. *Appl. Surf. Sci.* 2018. **459**: 171.